

E040 029

SPIN/NOI 17

(1)

# On the Introduction of Special Sensor Microwave Imager (SSM/I) Data into the Andes Acoustic Ambient Noise Model

OTIC  
JUNE 1984

**P. M. Smith**  
Remote Sensing Branch  
Ocean Sensing and Prediction Division  
Ocean Science Directorate

Approved for	
Publication	<input checked="" type="checkbox"/>
Classification	<input type="checkbox"/>
Exemption	<input type="checkbox"/>
Justification	

By \_\_\_\_\_  
Distribution/

Availability Codes

Avail. and/or special

QUALITY INSPECTED 1

A-1



Approved for public release; distribution is unlimited. Naval Oceanographic and Atmospheric Research Laboratory, Stennis Space Center, Mississippi 39529-5004.

## ABSTRACT

The Special Sensor Microwave Imager (SSM/I) provides nearly global data coverage relating to sea surface roughness once every 24 hours. A quadratic retrieval algorithm is developed that can retrieve foam coverage and rms wave slope statistics from the SSM/I data. I show how that roughness product can be interpreted as a sound source for ambient noise. The Ambient Noise Directional Estimation System (ANDES) is modified for demonstration purposes to accept the SSM/I data in the form of maps of rms wave slope. A crude transfer function, which relates wave slope to sound source intensity, is derived using historical sonobuoy ambient noise data. Presentation graphics software is developed that presents a computer console operator with a visual display of receiver location, transmission loss contours, and ANDES omnidirectional noise results overlaying the grey-scale map of rms wave slope used to force the model.

## ACKNOWLEDGMENTS

This work was supported by Program Element No. 63704N, LCDR W.A. Cook, Program Manager, Space and Naval Warfare Systems Command. Marla Helveston of Sverdrup Technology Inc. developed the graphics software for displaying the ANDES output on the imaging screen. Bill Renner of SAIC devoted a significant amount of time explaining various features of the ANDES model. Ed Chaika of ONR Detachment, Bay St. Louis supplied me with a copy of the ANDES model for this demonstration.

**On the Introduction of Special Sensor Microwave  
Imager (SSM/I) Data Into the ANDES  
Acoustic Ambient Noise Model**

**1. INTRODUCTION**

The Ambient Noise Directional Estimation System (ANDES) is a numerical model of acoustic noise propagation. It employs global data bases that include bottom loss, sound velocity profile, ocean depth, and shipping type and density data bases. The applicable frequency range of ANDES is from 30 to 1000 Hz.

Two sources of noise are treated: shipping and wind-generated noise. Present satellite systems lack the coverage, resolution, and data processing capabilities for the real time specification of ship densities on the world's oceans. Consequently, ANDES must rely on historical ship data in order to simulate the source of shipping noise. Wind-generated sources of noise, on the other hand, could be specified in near real time if the nature of the sources were known and satellite data were available that provided an estimate of wind-generated source strength. The Special Sensor Microwave Imager (SSM/I) can provide the necessary sound source density and strength data that ANDES requires for real time estimation of noise conditions at a specified geographic location.

ANDES presently uses a user-supplied local wind speed in order to specify the local wind-generated noise source intensity and a user-supplied distant wind speed for the specification of distant wind source level. This technical note describes a method whereby the distant wind noise sources are provided to ANDES as a spatially varying field based on recent satellite data rather than a single number representing wind speed averaged over an ocean basin. Additionally, the local noise field is specified by averaging satellite data over a 40 nmi x 40 nmi area. Finally, after ANDES is run, the satellite data is displayed on an imaging screen, together with sound loss contours obtained from ANDES and ANDES-predicted omnidirectional noise levels at the frequencies selected.

This note is organized as follows: Section 2 briefly describes the ANDES model, Section 3 briefly describes the SSM/I, Section 4 describes the development of a satellite algorithm to retrieve sea foam and root-mean-square (rms) wave slope from the SSM/I data, Section 5 describes, in detail, the modifications to ANDES, required to implement the fusion of satellite data into the model, Section 6 describes how rms wave slope distribution is converted to sound source level, and Section 7 presents a discussion and conclusions.

**2. A BRIEF DESCRIPTION OF ANDES**

A full technical description of ANDES is presented in Renner (1986). I

present, here, a short description of the model. Figure 1 is a schematic representation of the ambient noise problem. A sonobuoy receiver is deployed at some location at a given depth. Sound arrives at the sonobuoy transducer from all directions and all arrival angles. ANDES breaks up the azimuth and elevation angles into  $10^\circ$  sectors and calculates the noise received from these directions. In order to accomplish this ANDES uses a sub-model, ASTRAL, that predicts the transmission loss to a sound source location. ASTRAL marches out in range, collecting sources and attenuating the source levels according to the nature of the ray path between the source and the sonobuoy receiver. The transmission loss is a functional of bottom losses, sound velocity profiles, bottom depths, and sea surface conditions encountered along the path of the ray. Finally, the sound level from the various directions are summed at the transducer location. Both ANDES and ASTRAL are very sophisticated models, and the reader is referred to Renner (1986) for more detail.

### 3. A BRIEF DESCRIPTION OF THE SSM/I

The SSM/I is a multichannel scanning microwave radiometer sensor package that is installed on board the Defense Meteorological Satellite Program (DMSP) satellite bus. SSM/I employs 7 channels composed of 4 frequencies, 3 of which use two polarizations. Frequencies are 19, 22, 37, and 85 GHz. Only the three lowest frequencies are used in this analysis. The antenna beam describes a cone as it scans and data is collected during the segment of the scan that looks backward at the earth's surface. The spatial resolution of the data is 25 km and the swath width is about 1400 km. The satellite is in a polar orbit, executing approximately 14 orbits each day. This scheme results in near global coverage of the world's oceans in a 24-hr period. Data gaps are diamond shaped and periodic in longitude. A series of these gaps exist, centered at about  $22^\circ$  N and  $22^\circ$  S latitudes.

Data from the SSM/I is down-linked to the Fleet Numerical Oceanography Center (FNOOC) in Monterey, CA. Other operational sites possessing an SMQ-11 satellite receiving system, as well as R&D sites such as the Naval Oceanographic and Atmospheric Research Laboratory, are also capable of receiving the data.

### 4. ALGORITHM DEVELOPMENT

Present ocean SSM/I retrieval algorithms solve for the geophysical variables, integrated water vapor, integrated cloud water, wind speed, and rain rate. Algorithms for rain rate and water vapor are nonlinear whereas the algorithms for wind speed and cloud water are linear. The wind speed algorithm was originally based on a combination of the SSM/I's sensitivity to foam and to rms wave slope (Hollinger and Lo, 1983). Since each of these variables can

be related to wind speed, the wind speed can then be inferred from the SSM/I brightness temperatures ( $T_b$ 's). This theoretical model was later supplanted by an empirical linear model based on a comparison of  $T_b$ 's with data buoy records (Goodberlet et al., 1990).

For the purpose of forcing the ANDES model with data from the SSM/I, I derive sea foam fractional coverage and rms wave slope as separate quantities since each of these variables are more directly associated with the breaking of waves and, hence, the generation of acoustic noise by the wind (Urick, 1986). The rms wave slope is related to the number of waves breaking per unit time, per unit area since, according to Longuet-Higgins (1978), waves of steepness greater than .436 ( $\theta = 23.5^\circ$ ) will rapidly become unstable and break. The number of such waves present is a monotonic function of the rms wave slope. Sea foam is an obvious by-product of the breaking process.

In order that the proposed algorithm be applied globally, I expand the geophysical variables, WV (water vapor), CW (cloud water), WS (wave slope), FM (sea foam fraction), and SST (sea surface temperature) in a Taylor Series in the 5 low-frequency SSM/I channels:

$$\vec{G} = \vec{G}_0 + \frac{1}{n!} \{\mathcal{L}\}^n \vec{G} \quad (1)$$

where

$$\vec{G} = (WS \quad FM \quad CW \quad WV \quad SST),$$

and

$$\mathcal{L} = \vec{\delta} \cdot \nabla,$$

where

$$\vec{\delta} = (\Delta T_{19V} \quad \Delta T_{19H} \quad \Delta T_{22V} \quad \Delta T_{37V} \quad \Delta T_{37H}).$$

To second order,  $n=2$ , and

$$\vec{G} = \vec{G}_0 + \frac{\partial \vec{G}}{\partial \vec{T}_b} \vec{\delta} + \frac{1}{2} \frac{\partial^2 \vec{G}}{\partial \vec{T}_b^2} \vec{\delta}^2 \quad (2)$$

where  $\vec{G}_0$ ,  $\frac{\partial \vec{G}}{\partial \vec{T}_b}$ , and  $\frac{\partial^2 \vec{G}}{\partial \vec{T}_b^2}$  comprise 21 constants to be determined, for each component of  $\vec{G}$ .  $\vec{G}_0$  is the climatic mean corresponding to  $\vec{T}_0$ , the vector of average brightness temperatures from which  $\vec{\delta}$  is calculated:

$$\vec{\delta} = \vec{T} - \vec{T}_0.$$

By way of example,

$$\begin{aligned}
 WS = & A + B\Delta T_{19V} + C\Delta T_{19H} + D\Delta T_{22V} + E\Delta T_{37V} + F\Delta T_{37H} + G\Delta T_{19V}^2 \\
 & + H\Delta T_{19V}\Delta T_{19H} + I\Delta T_{19V}\Delta T_{22V} + J\Delta T_{19V}\Delta T_{37V} + K\Delta T_{19V}\Delta T_{37H} \\
 & + L\Delta T_{19H}^2 + M\Delta T_{19H}\Delta T_{22V} + N\Delta T_{19H}\Delta T_{37V} + O\Delta T_{19H}\Delta T_{37H} \\
 & + P\Delta T_{22V}^2 + Q\Delta T_{22V}\Delta T_{37V} + R\Delta T_{22V}\Delta T_{37H} + S\Delta T_{37V}^2 \\
 & + U\Delta T_{37V}\Delta T_{37H} + V\Delta T_{37H}^2.
 \end{aligned}
 \tag{3}$$

The coefficients are obtained through a least squares fitting of equation 2 to a set of synthetic data generated by a model of the radiation transport process. The model describes atmospheric emissions and absorption through the atmospheric transport mechanism described by Wisler and Hollinger (1977) and by Ulaby et al. (1981). The effect of a roughened sea surface is included using the model of emissions and reflections from the sea of Stogryn (1967). Finally, foam is modeled by an absorbing medium partially covering the sea surface and having emissivity of 1.0 at 37 GHz and .85 at 19 GHz. The foam emissivities were deduced from the measurements of Smith (1988).

The modeled climates are composed of most of the permutations in the following conditions:

TABLE I

WveSlope(m/s)	Foam Cover(%)	SST (°C)	Clouds	Climates
3	0	0	Clear	Tropical
6	2	5	Stratus	Mid-Lat-Sum
9	4	10	Cumulus	Mid-Lat-Win
12	6	15	Altostratus	Sub-Arc-Sum
15	8	20	Stratus-Cum's	Sub-Arc-Win
18	10	25	Nimbostrat	US Standard
		30		

Wave slope is expressed in units of velocity so that it can be readily related to the wind which would prevail if the waves were in equilibrium with the wind. Wave slope in units of *m/s* can be converted to the usual dimensionless units by using the formula published by Cox and Munk (1954):

$$\sigma^2 = 0.003 + 0.00512W,$$

where  $W$  is the wind velocity in  $m/s$  and  $\sigma$  is the rms value of the wave slope.

The following table lists the coefficients obtained through fitting the synthetic data set,  $\{\bar{G}\}$  to the set,  $\{\bar{T}\}$ , obtained from the model. I use the lettering convention employed in equation 3. The dominant coefficients are printed in bold type.

TABLE II

COEF	WS	FM	CW	WV	SST
A	9.32940	5.99879	.4602	21.2203	300.63
B	-.011475	-.366305	-.009534	-.148794	<b>3.5715</b>
C	<b>.118005</b>	<b>.786925</b>	<b>-.062664</b>	<b>.415040</b>	-1.3233
D	-.013709	<b>-.640511</b>	<b>.055111</b>	<b>.688625</b>	-.5917
E	<b>-1.284631</b>	<b>.705614</b>	-.025391	-.219701	-1.8829
F	<b>.646145</b>	-.477568	<b>.071107</b>	-.270702	.77550
G	.063106	-.035778	-.011952	.028638	<b>-.10896</b>
H	-.05805	-.014142	.007956	.047171	.00481
I	-.004639	.030289	.006150	<b>-.053532</b>	.075896
J	<b>-.151220</b>	.035348	<b>.022791</b>	.032856	.009667
K	.058327	.010723	<b>-.010496</b>	<b>-.047702</b>	.02458
L	-.007190	-.003696	.000476	.009687	-.01007
M	.019398	.008671	-.003233	-.015444	.00847
N	.039343	.004077	<b>-.015178</b>	-.058511	-.01417
O	.0137586	.006230	.001982	-.003286	.01799
P	-.002200	-.003741	-.001575	.014993	-.01997
Q	.013999	-.038156	.003831	.043333	.00637
R	-.018031	-.004570	.001633	.005390	-.01957
S	<b>.118961</b>	-.000530	<b>-.021322</b>	<b>-.069649</b>	.03472
U	-.070894	.010657	<b>.020617</b>	.070128	<b>-.00579</b>
V	.000698	-.008199	-.002302	-.003893	-.00704

The mean values for brightness temperature are calculated from the model runs and are shown in the table below:

TABLE III

$\bar{T}_{19V}$	$\bar{T}_{19H}$	$\bar{T}_{22V}$	$\bar{T}_{37V}$	$\bar{T}_{37H}$
203.811	148.720	22M.469	218.793	170.786

The rms deviation of the data from the model function (termed the "rms error") is displayed in the following table. Two cases are shown: with and without the inclusion of instrumental noise. The instrumental noise values were obtained from Hollinger et al. (1989).

TABLE IV  
RMS ERRORS

	WS(m/s)	FM(%)	CW(Kg/m <sup>2</sup> )	WV(Kg/m <sup>2</sup> )	SST (°C)
no noise	1.52	1.67		2.00	2.3
w/ noise	2.10	2.20	0.51	2.06	4.5

I restrict my attention to the Atlantic Ocean and apply the above algorithm to SSM/I  $T_b$ 's recorded over this region. An imaging system using International Imaging Systems software is used to process the SSM/I data. An ocean basin such as the Atlantic from 20°S to 80°N will fit conveniently in a 512 x 512 image at 20 km resolution. Figures 2 and 3 are images showing the result of applying the sea foam and wave slope algorithms to the data. Since the algorithm is quadratic in the  $T_b$ 's, when the set of  $T_b$ 's are outside of the range corresponding to realistic climate conditions, the geophysical retrievals often become either negative or very large. Therefore the identification of bogus retrievals becomes somewhat easier than in the case of the linear algorithm. For this data set I have mapped all negative values into maximum brightness (255). Anomalously high values, also, will appear in the grey scale image as being very bright.

Figure 2 is an image representation of the sea foam retrievals for 7 Dec 1988. Since the uncertainty in retrievals is (+/-) 2%, I display results for the range, -2% to above 5%. Almost all of the white colored regions are bogus retrievals. The high water vapor in the tropics and the vapor related to a storm located in the central Atlantic obscure the sea surface for the purpose of retrieving sea foam.

The remaining valid sea foam retrievals appear to represent approximately 50% of the North Atlantic. Hence, in spite of the obvious importance of sea foam as an indicator of the number of breaking waves present, the difficulties of accurately retrieving this quantity over a significant fraction of the sea appears to diminish its usefulness as an indicator of ambient noise. Faced with these difficulties with sea foam I turn to the rms wave slope retrievals. Figure 3 shows the wave slope data for 8 Dec 1988 and the retrievals appear to be much more reliable in this case. This shouldn't be too surprising since the SSM/I incident angle was set to  $53^\circ$  (the angle at which the vertically polarized channels are insensitive to wind) to maximize the accuracy of wind retrievals. The figure shows very few areas where obviously bad retrievals have occurred. These areas are restricted to what appears to be high precipitation areas. The anomalously high brightness areas do not correlate with maps (not shown) of water vapor concentration, but do appear to be well correlated with maps of cloud water. Since these anomalous regions will ultimately represent strong artificial sources of noise, they must be removed.

To this end, a blotched graphics plane is created, based on a threshold applied to the corresponding cloud water image. The corresponding pixels in the wave slope image are then set to zero. The wave slope image is then interpolated across these areas that have been forced to zero.

## 5. MODIFICATIONS TO THE ANDES MODEL

### Interfacing the Satellite Data to ANDES

The ANDES model, as presently configured, predicts wind-generated noise based on a user-supplied local wind speed (valid up to 40 nmi from the observation point) and a distant wind that is assumed to be constant over the remainder of the ocean basin (Renner, 1986). I treat the local wind noise much the same as the present configuration does. Satellite rms wave slope data is averaged over a square area, 100 km on a side, with the observation point at the center. This average slope is converted to source level and replaces the wind-derived source level, WINDSRC(K), in subroutine, LOCAL-WIND.

The distant wave-generated noise is treated differently from the present distant wind algorithm. The subroutine, WINDSD, is modeled after the subroutine, SHIPSD, which determines the shipping noise source density within a given  $10^\circ$  sector. As ASTRAL marches out in range for a particular sector, wave slope contributions to the noise are added similar to the way shipping noise is added. WINDSD retrieves the value of the rms wave slope from the satellite-derived rms wave slope for the range and sector under consideration. The rms wave slope is assumed to be related to the number of waves breaking per unit time, per unit area. The wave slope is multiplied by the area subtended by two

10° radials and two arc segments within the WINDSD subroutine, similar to the shipping density in the SHIPSD subroutine. The sound source in units of number of waves breaking per unit time is passed to the INTSUM subroutine in the ASTRAL model where it is converted to a source level.

Since distributed sources such as shipping noise must be set up in advance, the satellite data for an entire ocean basin is placed into the array, FOAMDAT, in subroutine, LOAD\_FOAM, in advance. LOAD\_FOAM is called by subroutine GET\_SOURCE. FOAMDAT is a real array representation of the grey-scale image created by the image processing system. Each pixel has dimensions .2° latitude by .2° longitude. WINDSD accesses the array, FOAMDAT, through the subroutine, GET\_FOAM. GET\_FOAM is similar to GET\_FOAM\_LCL, except that no averaging is performed in it.

For local wind, subroutine, GET\_FOAM\_LCL, scales and offsets the data in FOAMDAT and creates an average over a 5 pixel x 5 pixel area. This average is returned in the variable, FOAM\_FRAC, to subroutine, LOCAL\_WIND, where it is converted to a source level.

The subroutine, LOAD\_FOAM, accesses the satellite image through unit, ANDFOM. This channel is opened through an OPEN statement in the subroutine, OPEN\_USER. The filename of the image, 'ANDFOM', is assigned to the image file in the command file, ANDES2.COM.

#### Presenting the Data to the Imaging Screen at Conclusion of the Run

In order that a user might be able to evaluate the noise levels predicted by ANDES in terms of the quality of the satellite data used as input, ambient noise and satellite data were merged on the imaging screen following the execution of the ANDES run. An enhanced version of the rms wave slope data together with an 'X' denoting the observation point is displayed, as well as contours surrounding the observation point depicting the -150 dB, -70 dB, and -50 dB transmission loss. This transmission loss includes bottom scattering and absorption losses, and surface scattering losses. Losses not included in this figure are cylindrical spreading losses and source-to-mode coupling losses. Losses are maximum losses for any mode at the specified range.

The -150 dB loss contour defers to the equator, a land boundary or the 80° N latitudinal boundary if the track intersects such a boundary. These contours overlay the grey-scale satellite image in different colors and help the analyst to decide whether there will be a problem with the interpretation of the ANDES prediction vis' a' vis' anomalies in the satellite data. This information is stored in file, ANDMAP, during the ASTRAL integration and during the execution of the display routines. These data are retrieved by the imaging software from ANDMAP following the execution of ANDES. Another variant to the program allows the analyst to change the depth of the transducer interactively and rerun

the model.

The following changes were made to ANDES2 in order to implement the foregoing features:

1. Add file, FOAM.CMN,:

```
REAL*4 TOTL_FOAM(MAXDENS)
REAL*4 FOAMDAT(512,512)
REAL*4 FOAM_COEF(5)
```

```
COMMON /FOAM/ TOTL_FOAM, FOAMDAT, FOAM_COEF
DATA FOAM_COEF/3.24E5, 3.92E5, 3.92E5, 3.81E5, 2.308E5/
```

2. In GET\_SOURCE.FOR

add            INCLUDE 'FOAM.CMN'

after          IF(DIST\_IND\_FLAG),

add            CALL LOAD\_FOAM

change        CALL WINDSD(...., SRC\_DEN(1,8))  
to            CALL WINDSD(...., TOTL\_FOAM(1))

and then add DO J=1,NSTEPS  
              SRC\_DENS(J,8)=TOTL\_FOAM(J)  
              ENDDO

3. Modify subroutine SHIPSD, to become subroutine WINDSD as follows:

Change        SUBROUTINE SHIPSD(BEAR1,... )  
to            SUBROUTINE WINDSD(BEAR1, BEAR2, RANGE\_MAX,  
              NSTEPS, TOT\_FOAM)

Replace       REAL\*4 SHIP\_DENS(MAXDENS,6)  
with          REAL\*4 FRAC\_FOAM(MAXDENS)  
              REAL\*4 TOT\_FOAM(MAXDENS)

Replace the line, CALL ZILCH(SHIP\_DENS, 6\*MAXDENS)  
with          CALL ZILCH(FRAC\_FOAM, MAXDENS)  
              CALL ZILCH(TOT\_FOAM, MAXDENS)

Replace the line, CALL GET\_SHIP(XLAT, XLON, SHIPS)

with           CALL GET\_FOAM(XLAT, XLON, FM\_FRAC)

After           C ACCUMULATE AT PROPER RANGE  
I=NDEL\*(IR-1)+JR,

Replace        DO ITYPE =1, 6  
SHIP\_DENS( )= ...  
ENDDO

with           FRAC\_FOAM(I) = FRAC\_FOAM(I) +FM\_FRAC

After           DO JR= 1, NDEL  
I = NDEL\*(IR-1) +JR,

replace        DO ITYPE = 1,6  
SHIP\_DENS ( ) = ...  
ENDDO

with           IF (DEL\*1.E. RANGE\_LOCAL) THEN  
TOT\_FOAM(I) = 0.0  
ELSE  
TOT\_FOAM(I) = FRAC\_FOAM(I)\*AREA(JR)  
ENDIF

4. Introduce subroutine, GET\_FOAM.

See Appendix A for a listing.

5. Introduce subroutine LOAD\_FOAM.

See Appendix A for a listing.

6. In subroutine, INTSUM,

Add           INCLUDE '[-]FOAM.CMN'  
(assumes that ASTRAL resides in a subdirectory of ANDES)

Add           REAL\*4 AREA\_FACTOR  
Add           AREA\_FACTOR = (6076.1/3)\*\*2

Add, after comment,

C CALCULATE RUNNING SUM OF NODAL  
NOISE INTENSITY USING CURRENT HALF STEP,

DO N=1, NF

```
SRC_LEVEL(N,NUM_SRC_TYP) = FOAM_COEF(N)*  
AREA_FACTOR/PI  
ENDDO
```

(Note: In this demonstration version, NF is assumed to be 5.)

7. In subroutine MARCH,

```
Add          INCLUDE 'CONV.COM'  
  
In statement, LOGICAL DONE, FIRST, etc...,  
  
Add          FIRST2, FIRST3 to the list.  
  
After,       5 CONTINUE,  
  
Add          FIRST2 = .FALSE.  
            FIRST3 = .FALSE.  
  
After,       850 CONTINUE  
            C COMPUTE INTENSITY  
            CALL INTSUM,  
  
Add          IF(TLSUM*DZMIN1.LE.AMPMN3.AND.FIRST3  
            .EQ.FALSE) THEN  
            FIRST3 = .TRUE.  
            WRITE(ANDMAP) RANGE(IR)  
            END  
  
After, 1000 CONTINUE  
  
Add,         IF (FIRST2.EQ..FALSE.) THEN  
            WRITE(ANDMAP) RANGE(IR)  
            ENDIF  
  
            IF(FIRST3.EQ..FALSE.)THEN  
            WRITE(ANDMAP) RANGE(IR)  
            ENDIF  
  
            WRITE(ANDMAP) RANGE(IR)
```

8. In subroutine INITAL,

```
After, TLMAX = 150.0
```

Add TLMAX2 = 70.0  
TLMAX3 = 50.0

After, AMPMIN = 10.\*\*(-(TLMAX ...))

Add  
AMPMIN2 = 10.\*\*(-(TLMAX2-DBCONV)/10.)  
AMPMIN3 = 10.\*\*(-(TLMAX3-DBCONV)/10.)

9. In file, CONV.COM

Add to COMMON /CONV/ DBCONV, TLMAX, etc...

the variables, AMPMIN2, AMPMIN3

10. In subroutine AVER\_NOISE,

After, IF DIST\_WIND\_FLAG)  
READ(AND\_WDT) ANG1, ANG2, etc...

Add WRITE(ANDMAP) ANG1, ANG2

11. In subroutine OPEN\_USER,

After last OPEN statement,

Add  
OPEN( UNIT=ANDMAP, FILE=ANDMAP\_NAME, STATUS='NEW',  
RECORDTYPE='VARIABLE', FORM='UNFORMATTED')

OPEN( UNIT=ANDFOM, FILE=ANDFOM\_NAME, STATUS='OLD',  
FORM='UNFORMATTED')

12. In file, IOUNIT.PAR

Add INTEGER\*4 ANDMAP  
INTEGER\*4 ANDFOM  
CHARACTER\*6 ANDMAP\_NAME  
CHARACTER\*6 ANDFOM\_NAME  
PARAMETER (ANDMAP\_NAME='ANDMAP')  
PARAMETER (ANDFOM\_NAME = 'ANDFOM')  
PARAMETER (ANDFOM = 10)  
PARAMETER (ANDMAP = 39)

### 13. In subroutine AN\_DISPLAY

After REAL\*4 WIND

Add WRITE(ANDMAP) OPTION

After DO J = 1, NUM\_SRC\_TYP  
OMNI(J) = 10.ALOG10(AMAX1(1., OMNI(J)))  
ENDDO

Add WRITE(ANDMAP) FREQ(I), OPTION  
WRITE(ANDMAP) OMNI.TOTAL

## 6. INCORPORATING RMS WAVE SLOPE INTO ANDES

In the present version of ANDES, wind speed is the forcing function for wind-generated noise. Wind speed is related to sound source level in dB re  $1\mu\text{Pa}$  through the "Wenz" curves (Perrone, 1969) which were derived from experimental data.

Since there are no data relating rms wave slope to sound source level I hypothesize that the source level,  $S$ , is linearly related to the rms wave slope and has a frequency dependence similar to that of the Wenz curves, i.e.

$$S(f, WS) = a(f)WS$$

where  $f$  is frequency and  $WS$  is the rms wave slope.  $a(f)$  takes the form of 5 constants specified for each of the frequencies, 50, 100, 200, 440, and 1000 Hz. This model of wind-generated noise is consistent with the observation by Longuet-Higgins (1978) that, of the population of ocean waves present, those having wave slope greater than  $23^\circ$ , will become unstable and will eventually break. This population is represented by the area under the tails of the wave slope probability distribution function (pdf). The pdf has been shown to be closely approximated by a Gaussian distribution (Cox and Munk, 1954). Such a distribution is shown in Figure 4 with the shaded area denoting the population of unstable waves. A Gaussian pdf is completely specified by the mean value and the variance or rms value. The mean value for wave slopes must be zero and, hence, the rms wave slope completely specifies the distribution and, in particular, the population of unstable waves.

The rms wave slope is, therefore, monotonically related to the number of waves breaking per unit time, per unit area which, I postulate, is linearly related to the sound source level.

The values for  $a(f)$  must be estimated. I use historical sonobuoy data and compare these measured noise values with ANDES-predicted noise levels using

a candidate set of constants for  $a(f)$ . These values are then adjusted in order to achieve the best fit to the data.

The sonobuoy data were taken from the FNOC master ambient noise data base, and included approximately 100 sonobuoy drops. Using the observed wind speeds (which were reported with the sonobuoy data) I ran the ANDES model to determine whether shipping noise was likely to overwhelm wind-generated noise for a given situation, at least above 100 Hz. After excluding those cases in which there were high ambient noise levels due to shipping, the number of cases was reduced to 27. Lack of good, coincident (within 24 hrs) satellite data reduced this number to 14.

The number of data points was further reduced to 7 due to observation points lying within one of the diamond-shaped regions not covered by the SSM/I data coverage or for other reasons.

The 5 constants,  $a(f)$ , were adjusted, first, so that agreement in local wind noise for one of the 7 cases was achieved. The model was then run for all 7 cases and the results are shown in Figure 5. The predictions over-predict the value of the noise in each case. This is to be expected at the lower frequencies since we intentionally excluded cases with high shipping noise contributions. However noise levels at 1000 Hz should be dominated by local wind effects and agreement should be better at that frequency. The constants,  $a(f)$ , were then reduced in magnitude, proportionately, in order to minimize the variance of the predicted versus the measured data points about the 45° regression line at a frequency of 1000 Hz. The results from this adjustment are shown in Figure 6. The over-predictions have been greatly reduced except at 50 Hz where we expect shipping noise to remain the dominant contributor to the predicted noise. Final values for  $a(f)$  are shown in the table below.

TABLE V

<u>a(1)</u>	<u>a(2)</u>	<u>a(3)</u>	<u>a(4)</u>	<u>a(5)</u>
3.24E5	3.92E5	3.92E5	3.81E5	2.308E5

In order that an operator can interpret the results of the ANDES analysis with regard to the satellite data used as input to the model, the model output is presented to the console operator as graphics overlaying an image of the satellite data used as input. Figures 7 and 8 are examples of what the console operator would see after the model run is over. Figure 7 is a display resulting from a receiving transponder having been located in the North Atlantic south of Iceland. The receiver depth is 400 ft. As can be seen by the 70 dB loss contour, sound sources in the South Atlantic travel unimpeded to the receiving transponder.

Sound originating in the Greenland Sea, however, cannot cross the Iceland-Faroes ridge. Figure 8 shows a case of the receiver having been located in the Greenland Sea. Most of the sound arriving at the transducer originates in the Greenland Sea.

Most of the wind noise in the North Atlantic is associated with a low pressure system and its related fronts. The black diamonds are data-void areas and do not contribute to the ambient noise estimate. Today, these diamond-shaped regions would be partially filled in with data from a combination of the two SSM/I's now in orbit.

## 7. DISCUSSION

A method of incorporating SSM/I data into the ANDES ambient noise model has been demonstrated. A simple model for translating rms wave slope to sound source level, for the purpose of driving the ANDES model, has also been proposed. Since surface truth for rms wave slope is difficult to obtain (See Smith and McCardle, 1990 for an example), verification of the assumptions made must depend on comparisons of modeled noise levels with measurements. Only seven such measurements were available for this technical note. More comparisons are obviously needed.

The nonsynoptic nature of the wave data is of some concern. Waves and wind are rapidly changing over the ocean surface and a 24-hr composite could not be considered synoptic for any purpose. A second SSM/I has been recently launched and data similar to what has been described here is now available for a 12-hr time interval rather than the 24-hr interval that was previously available.

A number of sonobuoy test cases had to be rejected because the corresponding SSM/I data was not of a sufficiently high quality to use. The data from SSM/I has significantly improved since the 1988 time frame when these data were collected. Hence, more good comparisons are now possible.

Since satellite data is not forecast data, but very recent data, the infusion of SSM/I data into a model such as ANDES must be viewed as diagnostic rather than predictive. Such a model is valuable at a field site where analysis of present conditions is necessary in order to decide whether or not deployment of resources such as sonobuoys or arrays is likely to be fruitful.

The computer code modifications prescribed in Section 4 and in Appendix A were tailored to an application in the Atlantic. Hence the code is not general enough, as presently configured, to handle the Pacific and Indian Oceans. Expansion of the present configuration to handle the additional ocean areas represents a relatively small effort, however.

The graphics coding was performed on an *I<sup>2</sup>S* Model 75 imaging system and is in general not portable to another imaging system. Implementation of similar software on a SUN workstation, for example, would be a relatively straightforward task.

## REFERENCES

- Cox, C.S. and W.H. Munk (1954). Measurements of the Roughness of the Sea Surface from Photographs of Sun Glitter. *J. of Am. Optical Society* 44:838-850.
- Goodberlet, M.A., C.T. Swift, and J.C. Wilkerson (1990). Ocean Surface Wind Speed Measurements of the Special Sensor Microwave Imager (SSM/I). *IEEE Trans. Geosci. Remote Sensing* 28:823-828.
- Hollinger, J.P. et al. (1989). DMSF Special Sensor Microwave/Imager Calibration/Validation Final Report Volume I. Naval Research Laboratory, Washington, D.C.
- Hollinger, J.P. and R.C. Low (1983). SSM/I Project Summary Report. NRL Memorandum Report 5055, Naval Research Laboratory, Washington, D.C.
- Longuet-Higgins, M.S. (1978). The instabilities of gravity waves of finite amplitude in deep water. I Superharmonics. *Proc. Royal Soc. London* A360:471-488.
- Perrone, A.J. (1969). Deep-Ocean Ambient Noise Spectra in the Northwest Atlantic *JASA* 46:762.
- Renner, W.W. (1986). Ambient Noise Directionality Estimation System (ANDES) Technical Description. SAIC Report 86/1645, Scientific Applications International Corp., Mclean, VA.
- Smith, P.M. (1988). The Emissivity of Sea Foam at 19 and 37 GHz. *IEEE Trans. Geos. and Remote Sens.* 26:541-547.
- Smith, P.M. and G.D. McCardle (1990). A Spar Buoy Design for the Measurement of Centimeter-Scale Waves in the Deep Ocean. *Proceedings of Oceans '90* Washington, D.C.
- Stogryn, A. (1967). The Apparent Temperature of the Sea at Microwave Frequencies. *J. Geophys. Res.* 77:658-1666.
- Ulaby, F.T., R.K. Moore, and A.K. Fung (1981). *Microwave Remote Sensing Active and Passive I* Addison-Wesley.
- Urlick, R.J. (1984). *Ambient Noise in the Sea*. Peninsula Publishing, Los Altos, CA.

Wisler, M.M. and J.P. Hollinger (1977). Estimation of Marine Environmental Parameters Using Microwave Radiometric Remote Sensing Systems. NRL Memorandum Report 3661, Naval Research Laboratory, Washington, D.C.

## APPENDIX A

```

SUBROUTINE GET_FOAM( ALAT, ALON, FOAM)

IMPLICIT NONE
INCLUDE 'ANDES.PAR'
INCLUDE 'FOAM.CMN'

C
REAL ALAT, ALON
REAL FOAM, BIAS, SCALE
REAL DEG_PIXEL, MAX_LAT, MIN_LON
INTEGER*4 LAT_INDEX, LON_INDEX

C
LOCAL VARIABLES
C
ALAT, ALON ! LOCATION FOR WHICH % FOAM IS DESIRED.
C
DEG_PIXEL ! SPACING BETWEEN FOAM DATA IN FOAMDAT.
C
LAT_INDEX ! INDICES FOR THE NEAREST NEIGHBOR GRID
C
LON_INDEX ! POINTS IN THE FOAMDAT ARRAY.
C
MAX_LAT ! NORTHERN BOUNDARY ON IMAGE ARRAY.
C
MIN_LON ! WESTERN BOUNDARY ON IMAGE ARRAY
C
BIAS ! OFFSET IN COUNTS USED TO CREATE FOAM IMAGE.
C
SCALE ! SCALE FACTOR USED TO CREATE FOAM IMAGE.
C

DATA DEG_PIXEL/0.2/
DATA MAX_LAT/80.0/
DATA MIN_LON/280.0/
DATA BIAS/10.0/
DATA SCALE/5./

C
FIND NEAREST NEIGHBOR GRID POINT IN IMAGE ARRAY.
C
LAT_INDEX = NINT( (MAX_LAT - ALAT)/DEG_PIXEL ) + 1

C
TEST FOR LONGITUDE BETWEEN GREENWICH AND LEFT EDGE OF
C
IMAGE.

IF(ALON.LT.MIN_LON) ALON=ALON+360.

LON_INDEX = NINT( (ALON - MIN_LON)/DEG_PIXEL ) + 1

C
RETRIEVE FRACTIONAL FOAM COVERAGE
C
FOAM = (FOAMDAT( LON_INDEX, LAT_INDEX )-BIAS)/SCALE
IF (FOAM.LT.0.0) FOAM=0.0
RETURN
END

```

```

SUBROUTINE LOAD FOAM
C PROGRAM READS IMAGE DATA WHICH HAS BEEN CONVERTED TO AN INTEGER
C FILE USING THE I2S FUNCTION, CPU'DISKTRANSFER AND FILLS ARRAY
C FOAMDAT.

INCLUDE 'ANDES.PAR'
INCLUDE 'FOAM.CMN'
INCLUDE 'IOUNIT.PAR'

INTEGER*2 Ibuff(256,512), MM, MM1, MM2, KK
DO 20 J=1, 512
READ (ANDFOM) (IBUFF(I,J), I=1, 256)
20 CONTINUE
KK=8
DO 10 J=1, 512
DO 10 I=1, 256
MM=IBUFF(I,J)
MM1=ISHFT(MM, KK)
MM2=ISHFT(MM1, -KK)
FOAMDAT(I*2-1, J)=MM2
MM1=ISHFT(MM, -KK)
FOAMDAT(I*2, J)=MM1
10 CONTINUE
RETURN
END

```

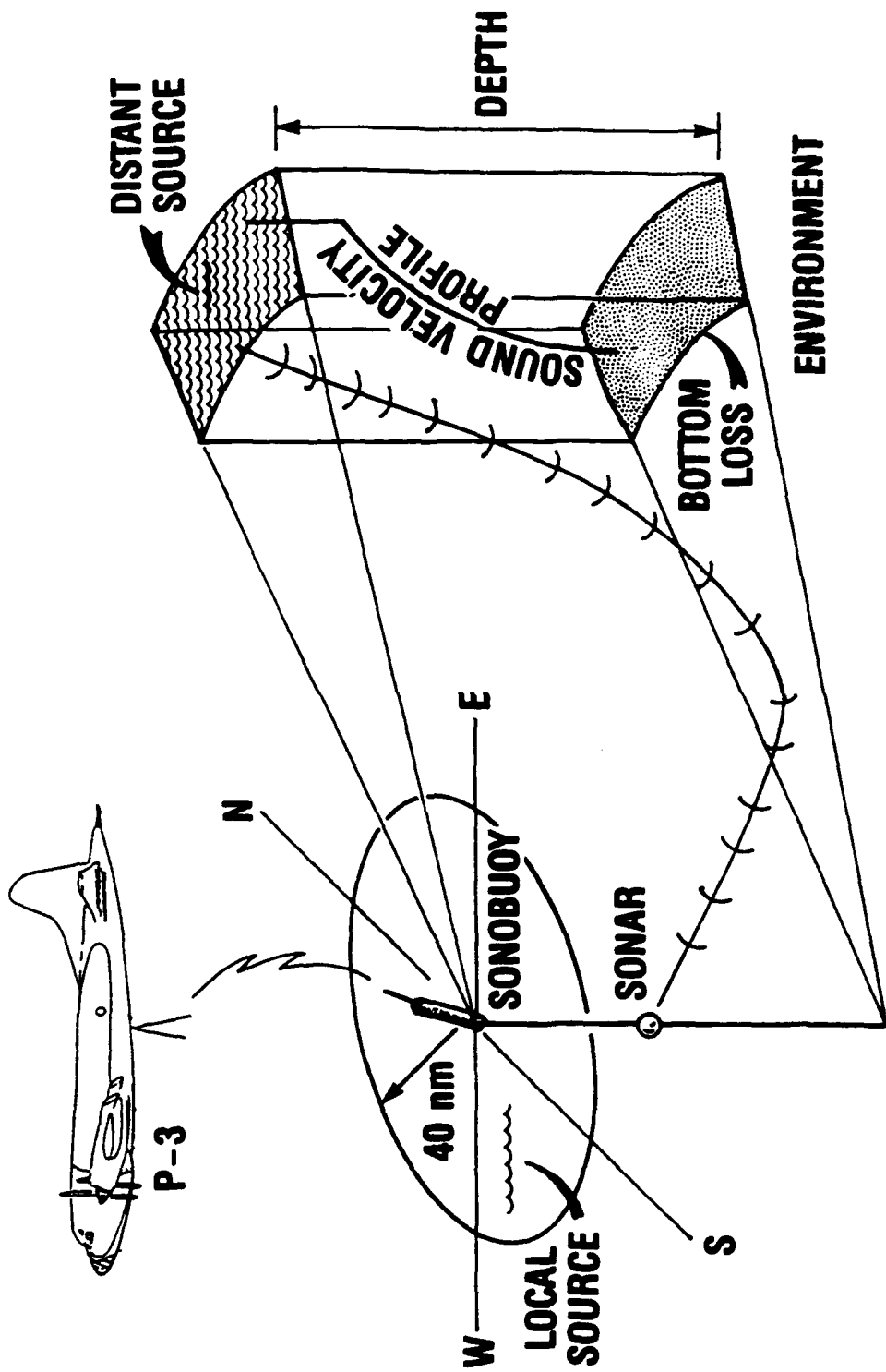


Figure 1. Schematic of ambient noise problem. ANDES integrates sources weighted by transmission loss as it marches radially from the transducer location. Environments are characterized by sound velocity profile, bathymetry, and bottom loss.



Figure 2. Percent foam coverage for the Atlantic Ocean basin as derived from applying quadratic retrieval algorithm to SSM/I data. White areas are bogus retrievals resulting from high water vapor concentration.

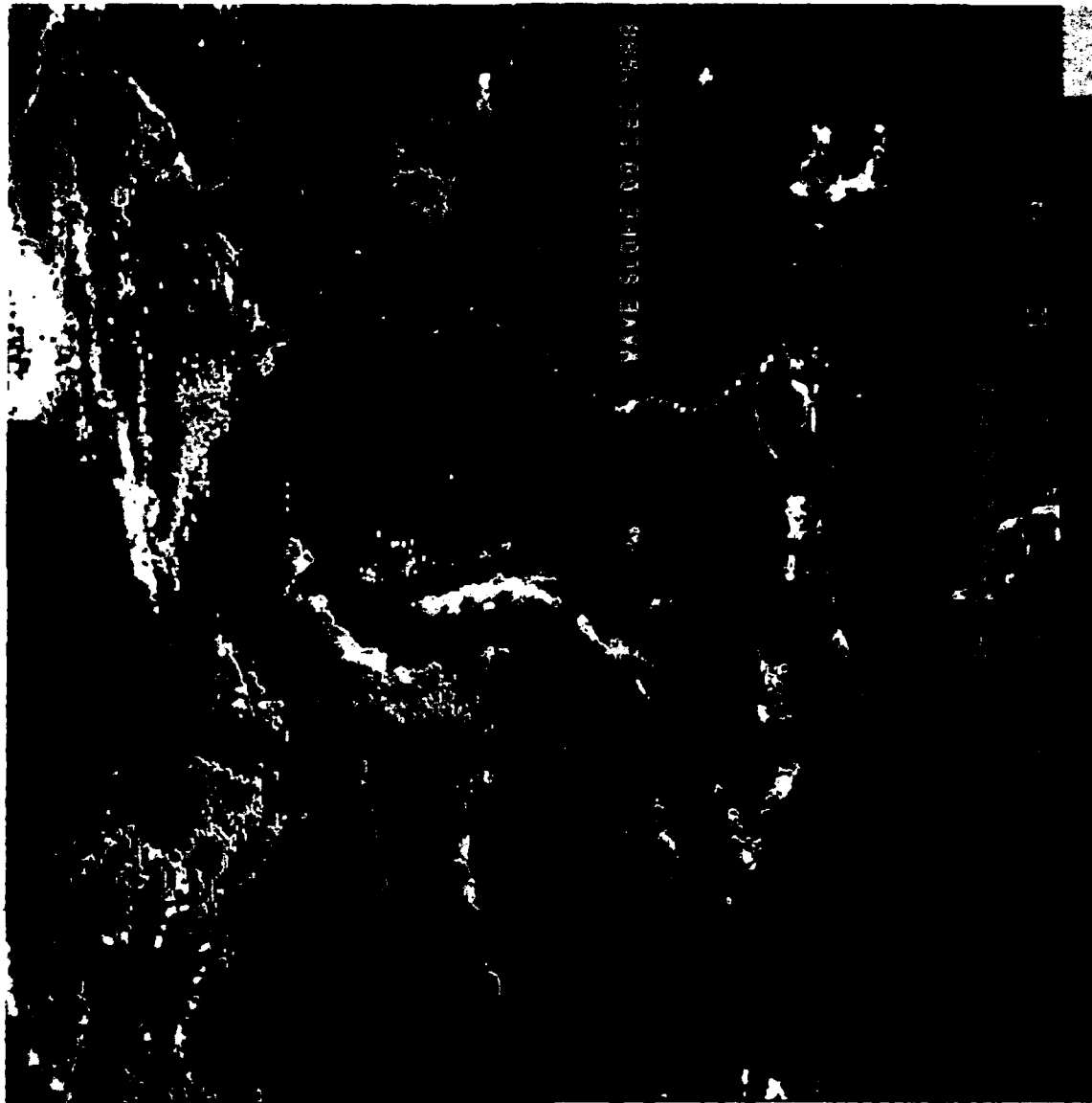
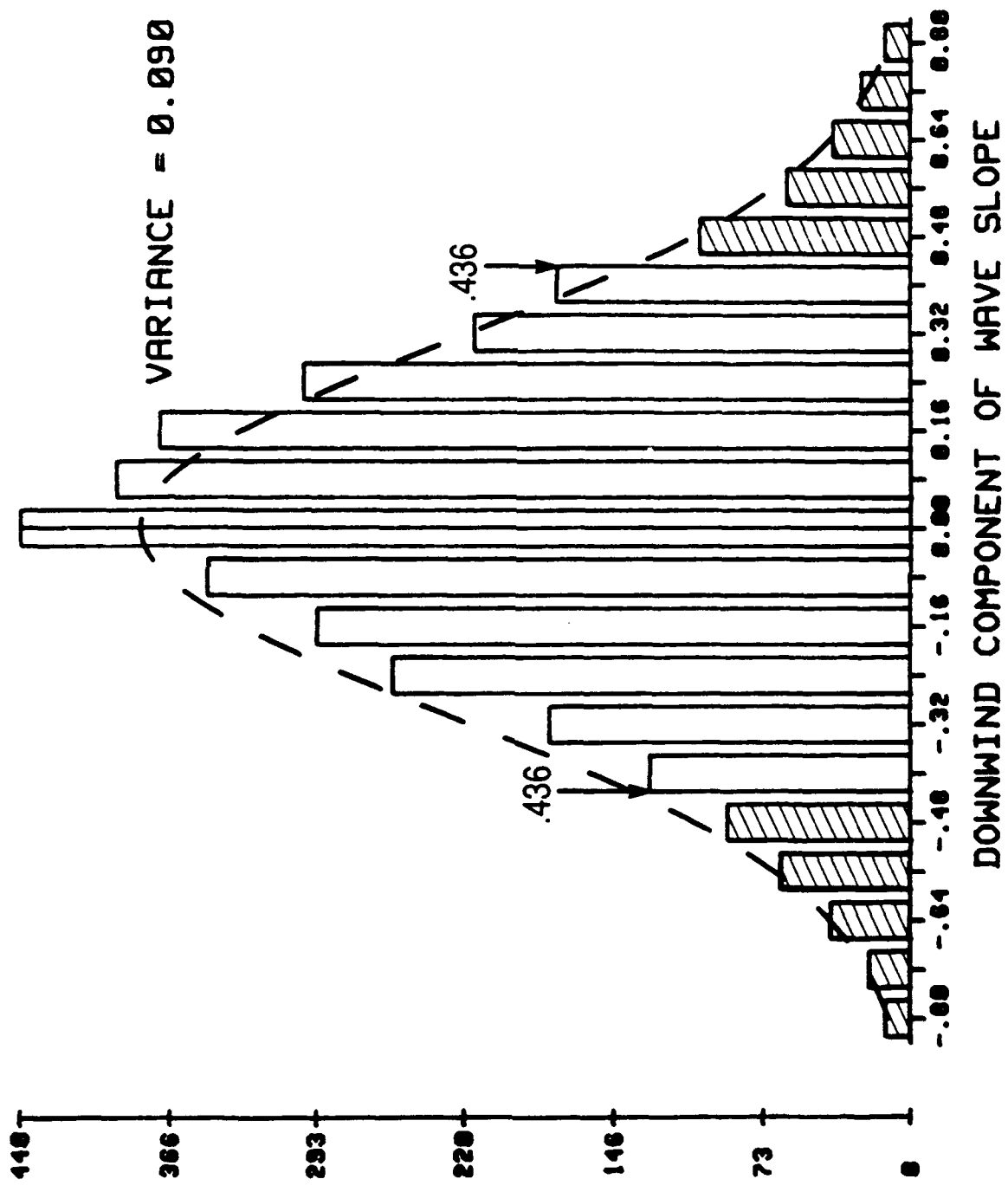


Figure 3. RMS wave slope for the Atlantic Ocean basin derived by applying quadratic retrieval algorithm to SSM/I  $T_b$ 's. Valid retrievals are possible for most of the ocean. Black diamonds are areas not covered by the 24 hour mosaic of ground swaths.



**DOWNWIND COMPONENT OF WAVE SLOPE**

Figure 4. Wave slope probability density function measured by Smith and McCardle (1990). Dashed line is Gaussian distribution having same variance as sample distribution. Shaded area under the curve represents population of unstable waves.

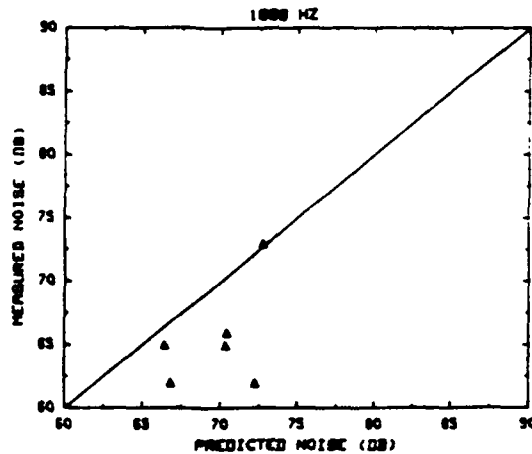
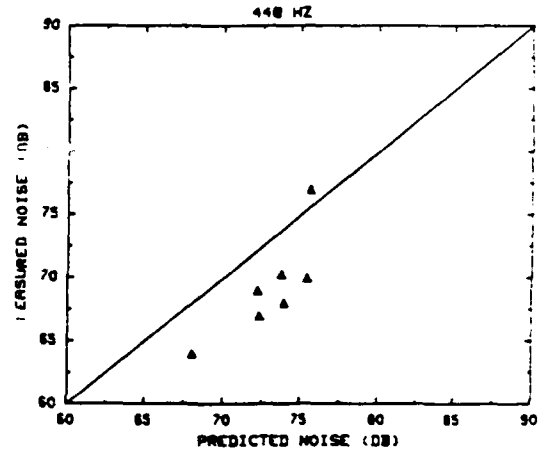
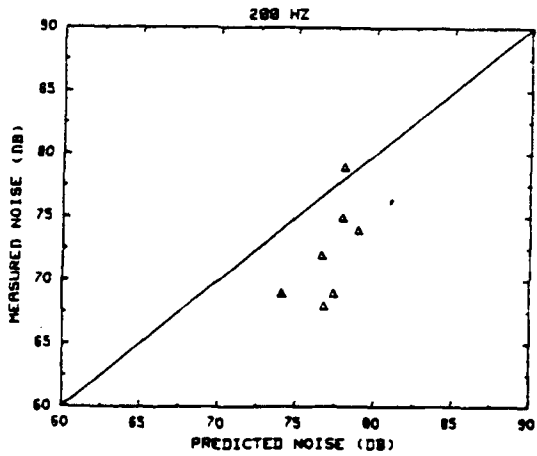
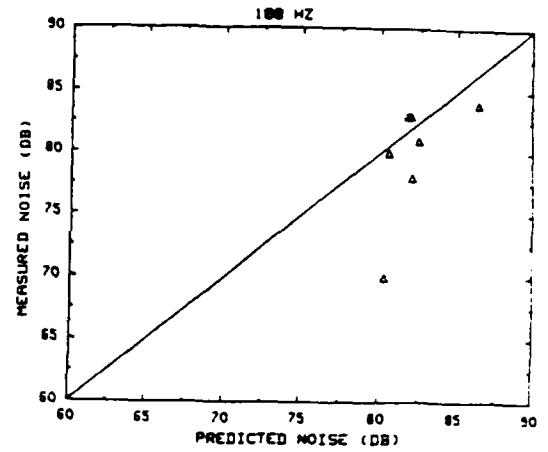
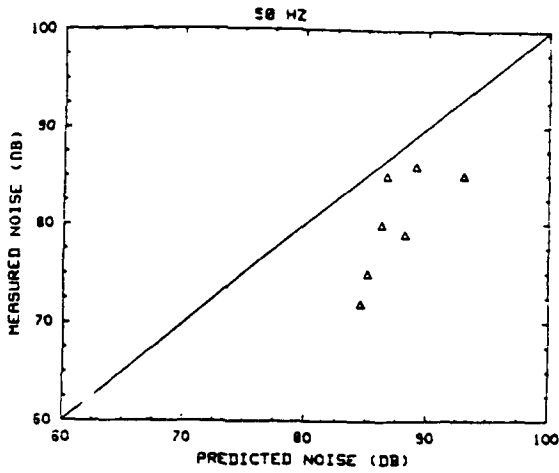


Figure 5. Regression plot of measured ambient noise versus ANDES/SSMI-predicted noise. Most values are over-predicted. Errors at 1000 Hz are due to errors in estimating the wave slope/wind noise sound source transfer function,  $a(f)$ .

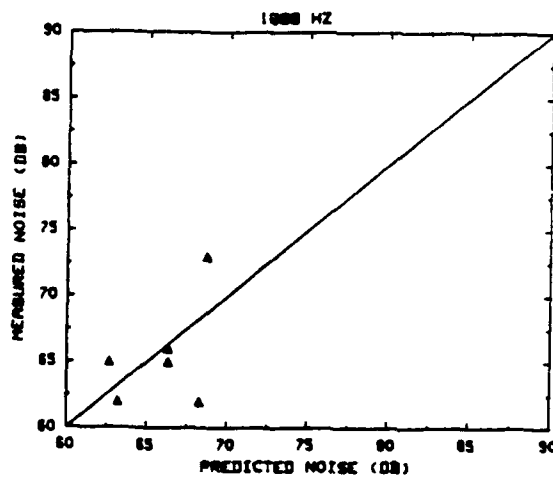
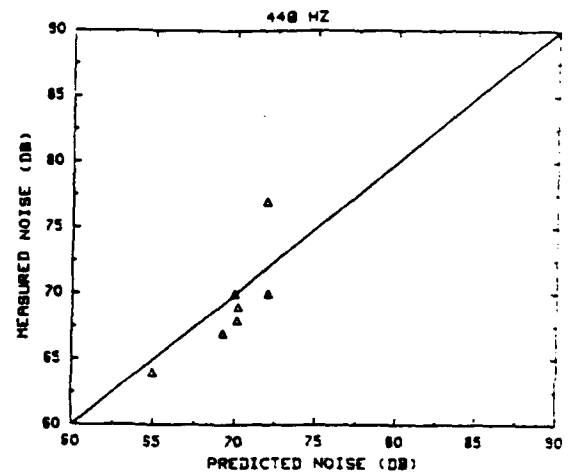
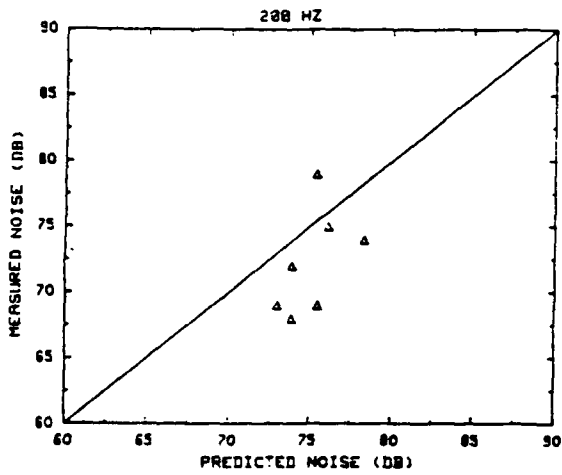
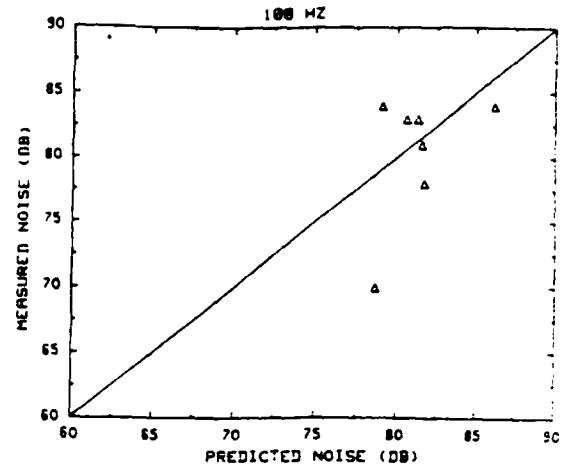
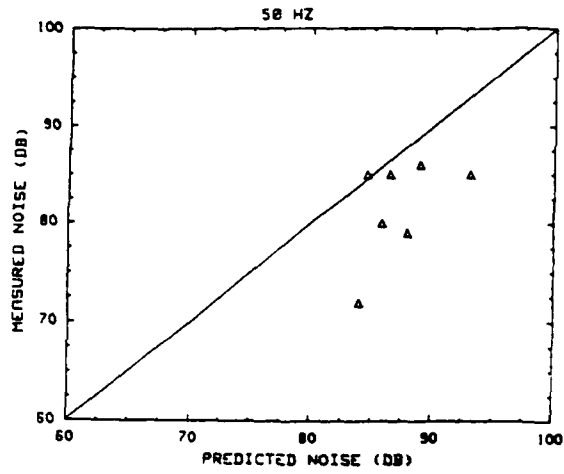


Figure 6. Regression plot of measured ambient noise versus ANDES/SSMI-predicted noise. The wave slope/wind noise sound source transfer function,  $a(f)$ , has been adjusted to reduce the variance of points about the regression line at 1000 Hz.



Figure 7. ANDES omnidirectional noise results superimposed on grey scale map of rms wave slope in the North Atlantic. Receiver is shown located south of Iceland. Contour lines show that -70 dB transmission loss area covers most of the Atlantic.



Figure 8. ANDES omnidirectional noise results superimposed on grey scale map of rms wave slope in the North Atlantic. Receiver is located in the Greenland Sea west of Norway. Note the lack of significant penetration of sound from the North Atlantic.

## DISTRIBUTION

Space and Naval Warfare Systems Command  
2511 Jeff Davis Highway  
Washington, D.C. 20363-5100  
ATTN: LCDR William Cook

Naval Oceanographic and Atmospheric Research Laboratory  
Stennis Space Center, MS 39529  
ATTN: Code 300  
Code 330  
Code 320  
Code 321  
Code 224 (Mr. Bruce Northridge)  
Code 224 (Mr. Robert Delgado)  
Code 245 (Dr. Ron Wagstaff)  
Code 245 (Dr. Joel Newcombe)  
Code 245 (Mr. Hassan Ali)  
Code 125L (6)  
Code 125P

Office of Naval Research Detachment  
Stennis Space Center, MS 39529  
ATTN: Mr. E.D. Chaika

Office of the Oceanographer of the Navy  
Naval Oceanography Division (OP-952)  
34th & Massachusetts Ave, NW  
Washington, D.C. 20390  
ATTN: Mr. Donald Montgomery

Scientific Applications International  
1710 Goodridge Drive  
McLean, VA 22102  
ATTN: Mr. William Renner

# REPORT DOCUMENTATION PAGE

Form Approved  
OBM No. 0704-0188

Public reporting burden for this collection of information is estimated to average 1 hour per response, including the time for reviewing instructions, searching existing data sources, gathering and maintaining the data needed, and completing and reviewing the collection of information. Send comments regarding this burden or any other aspect of this collection of information, including suggestions for reducing this burden, to Washington Headquarters Services, Directorate for Information Operations and Reports, 1215 Jefferson Davis Highway, Suite 1204, Arlington, VA 22202-4302, and to the Office of Management and Budget, Paperwork Reduction Project (0704-0188), Washington, DC 20503.

1. Agency Use Only (Leave blank).	2. Report Date. April 1991	3. Report Type and Dates Covered. Final
-----------------------------------	-------------------------------	--

4. Title and Subtitle. On the Introduction of Special Sensor Microwave Imager (SSM/I) Data into the Andes Acoustic Ambient Noise Model	5. Funding Numbers. Program Element No. 63704N Project No. 00101 Task No. 100 Accession No. DN258025
---	--

6. Author(s). P. M. Smith	7. Performing Organization Names(s) and Address(es). Naval Oceanographic and Atmospheric Research Laboratory Ocean Science Directorate Stennis Space Center, Mississippi 39529-5004	8. Performing Organization Report Number. NOARL Technical Note 120
------------------------------	--	---

9. Sponsoring/Monitoring Agency Name(s) and Address(es). Space and Naval Warfare Systems Command PMW-141 Washington, DC 20363-5100	10. Sponsoring/Monitoring Agency Report Number. NOARL Technical Note 120
---	---

11. Supplementary Notes.
--------------------------

12a. Distribution/Availability Statement. Approved for public release; distribution is unlimited.	12b. Distribution Code.
--	-------------------------

13. Abstract (Maximum 200 words). <p>The Special Sensor Microwave Imager (SSM/I) provides nearly global data coverage relating to sea surface roughness once every 24 hours. A quadratic retrieval algorithm is developed that can retrieve foam coverage and root-mean-square (rms) wave slope statistics from the SSM/I data. I show how that roughness product can be interpreted as a sound source for ambient noise. The Ambient Noise Directional Estimation System (ANDES) is modified for demonstration purposes to accept the SSM/I data in the form of maps of rms wave slope. A crude transfer function, which relates wave slope to sound source intensity, is derived using historical sonobuoy ambient noise data. Presentation graphics software is developed that presents a computer console operator with a visual display of receiver location, transmission loss contours, and ANDES omnidirectional noise results overlaying the grey-scale map of rms wave slope used to force the model.</p>
--

14. Subject Terms. Passive Microwave, Sea Ice, Water Vapor, Ambient Noise	15. Number of Pages. 25
--	----------------------------

17. Security Classification of Report. Unclassified	18. Security Classification of This Page. Unclassified	19. Security Classification of Abstract. Unclassified	20. Limitation of Abstract. SAR
--	---	--	------------------------------------

16. Price Code.
-----------------

17. Security Classification of Report. Unclassified	18. Security Classification of This Page. Unclassified	19. Security Classification of Abstract. Unclassified	20. Limitation of Abstract. SAR
--	---	--	------------------------------------

17. Security Classification of Report. Unclassified	18. Security Classification of This Page. Unclassified	19. Security Classification of Abstract. Unclassified	20. Limitation of Abstract. SAR
--	---	--	------------------------------------

17. Security Classification of Report. Unclassified	18. Security Classification of This Page. Unclassified	19. Security Classification of Abstract. Unclassified	20. Limitation of Abstract. SAR
--	---	--	------------------------------------